Surface Structure and Energetics of Hydrogen Adsorption on the Fe(111) Surface

Chun-Fang Huo,[†] Yong-Wang Li,[†] Jianguo Wang,[†] and Haijun Jiao*[,†,‡]

State Key Laboratory of Coal Conversion, Institute of Coal Chemistry, Chinese Academy of Sciences, Taiyuan 030001, P.R. China, and Leibniz-Institut für Organische Katalyse an der Universität Rostock e.V., Albert-Einstein-Strasse 29a, 18059 Rostock, Germany

Received: April 13, 2005; In Final Form: May 26, 2005

Spin-polarized density functional theory calculations have been performed to characterize the hydrogen adsorption and diffusion on the Fe(111) surface at 2/3-, 1-, and 2-monolayer (ML) coverages. It is found that the most favored adsorption site for atomic hydrogen (H) is the top-shallow bridge site (tsb), followed by the quasi 4-fold site (qff) with the energy difference of about 0.1 eV, while the top site (t) is not competitive. Furthermore, the adsorbed atomic hydrogen (H) has a high mobility, as indicated by the small diffusion barriers. The local density of state (LDOS) analysis reveals that the Fe−H (tsb or qff) bond involves mainly the Fe 4s and 4p and H 1s orbitals with less contribution of the Fe 3d orbital, while the Fe 4s, 4p, and 3d orbitals all participate in the Fe−H (top) bond. In addition, the coverage effects on the adsorption configurations and adsorption energies are addressed.

1. Introduction

The interaction of hydrogen with transition-metal surfaces is of great fundamental and practical importance in heterogeneous catalysis, metallurgy, energy storage, and fuel cell technology.[1−7] Since iron is an active phase for hydrogenation and dehydrogenation processes, iron-based catalysts are widely used in the Fischer−Tropsch reaction[8] and ammonia synthesis.[9] In addition, hydrogen is known to embrittle steels, causing fracture and ultimately failure of the steel component.[10,11] Therefore, hydrogen adsorption on Fe surfaces has attracted considerable attention.

Hydrogen is found to adsorb dissociatively on the low-index Fe surfaces, and the process is highly exothermic.[12−15] For the closest-packed (110) surface of body-centered-cubic (bcc) Fe, the low-energy electron diffraction (LEED) experiments indicated that H prefers to adsorb at the quasi 3-fold site.[15−17] However, early theoretical studies gave contradictory conclusions about the H site occupancy, such as the long-bridge site,[18,19] short-bridge site,[20] and quasi 3-fold site.[21,22] By using the spin-polarized density functional theory (DFT), Jiang and Carter[23] characterized atomic hydrogen adsorption on Fe(110); they found that the quasi 3-fold site is the only stable minimum, while the long-bridge and short-bridge sites are the transition states for H diffusion. For the close-packed Fe(100) surface, electron energy loss vibrational spectra[24] indicated that H prefers the 4-fold hollow site, in agreement with the early Hartree−Fock cluster prediction by Walch.[25] However, periodic DFT-GGA calculations by Eder et al.[26] suggested that H favors the 2-fold bridge site on Fe(100), and the 4-fold hollow site is slightly higher in energy. Recently, a very detailed spin-polarized DFT study on H/Fe(100) by Jiang and Carter[27] showed that a H adatom at the 4-fold hollow site is most stable, and that both the 2-fold bridge and the 4-fold hollow sites are true minima, while the on-top site is a rank-2 saddle point. Unlike Fe(110) and Fe(100), Fe(211) has a relatively open surface, but with close-packed rows. Hydrogen adsorption on Fe(211) shows a geometrical picture of zigzag chains with the H adatom at the 3-fold coordinated site.[3,28]

Although Fe(111) is thought to have high catalytic activity from the very open surface structure,[29] the related studies of hydrogen adsorption on Fe(111) are quite few. So far, it is not clear about the hydrogen adsorption sites on Fe(111). By means of low-energy electron diffraction (LEED), thermal desorption spectroscopy (TDS), work function measurements, and ultraviolet photoelectron spectroscopy (UPS), hydrogen adsorption on the Fe(111) single-crystal planes was investigated by Bozso et al.[12] It was found that hydrogen adsorption on Fe(111) forms a covalent H−Fe bond via coupling the H 1s state to the Fe valence states. The TDS experiments showed three peaks of the second-order desorption, β_1, β_2, and β_3, corresponding to the desorption temperature of 220, 300, and 360 K, respectively. However, the different desorption states with particular configurations on the very open Fe(111) surface cannot be identified by LEED. Several years later, Bernasek et al.[30] applied the thermal energy atom scattering (TEAS) technique to this interesting system and developed a model about the hydrogen adsorption sites. This model assumes different effective cross sections for H atoms adsorbed in the deep-hollow, the shallow-hollow, and the on-top or exposed sites. Furthermore, they suggested that these sites and cross sections might be related to the β_3, β_2, and β_1 peaks in the TDS data of Bozso et al.[12] The TEAS data also indicated the mobility of the adsorbed H atoms from the tightly bound deep-hollow site to the more weakly bound and higher cross-section adsites as the surface is warmed, in agreement with the finding of the work function experiments.[12] In addition, the sticking coefficients of adsorption system H_2/Fe were determined by nozzle beam experiments.[31]

In this paper, we present a systematic DFT study of hydrogen adsorption on Fe(111) at various coverages. The aim is to develop a detailed picture of the surface structure and energetics of the H_2/Fe(111) system, and further to elucidate the hydrogen adsorption states and sites as well as their diffusion. It is found that the most favored hydrogen adsorption on Fe(111) is

* Corresponding author. E-mail: haijun.jiao@ifok-rostock.de.
[†] Institute of Coal Chemistry, Chinese Academy of Sciences.
[‡] Leibniz-Institut für Organische Katalyse an der Universität Rostock e.V.

10.1021/jp051907s CCC: $30.25
Published on Web 07/01/2005

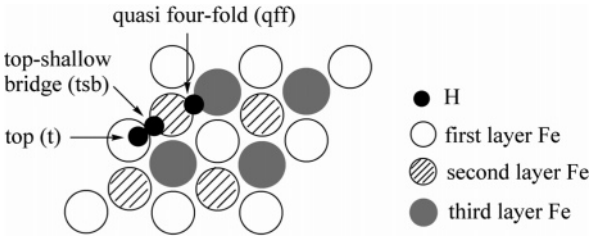

Figure 1. H atom adsorption sites on Fe(111).

dissociated. As shown in Figure 1, there are three adsorption sites for H atom, that is, the top site (t), the top-shallow bridge site (tsb), and the quasi 4-fold site (qff).

2. Methods and Models

2.1. Methods. All calculations were performed at the DFT level with the CASTEP program[32] in the Materials studio of Accelry Inc. The exchange and correlation energies were calculated using the Perdew, Burke, and Ernzerhof (PBE) functional[33] within the generalized gradient approximation (GGA).[34] Ionic cores were described by the ultrasoft pseudopotential,[35] and the Kohn−Sham one-electron states were expanded in a plane wave basis setup to 340 eV. A Fermi smearing of 0.1 eV was utilized to evaluate occupation numbers. Because of its large effect on the adsorption energies for magnetic systems,[36] spin-polarization was included in the calculations for a system with Fe. The convergence criteria for structure optimization and energy calculation were set to FINE with the tolerance for SCF, energy, maximum force, and maximum displacement of 1.0×10^{-6} eV/atom, 1.0×10^{-5} eV/atom, 0.03 eV/Å, and 1.0×10^{-3} Å, respectively. The complete linear synchronous transit/quadratic synchronous transit (LST/QST) method was used to locate the transition states for hydrogen diffusion.

Although the PBE functional can give reliable optimized geometry, it tends to overbind adsorbate on the metal surface.[37] In the PBE parametrization,[33] the parameter κ, which determines the degree of nonlocality of the GGA, is chosen so as to satisfy the Lieb−Oxford bound on the exchange energy for all possible electron densities ($\kappa = 0.804$). However, it is observed that the adsorption energies for a number of atoms and molecules on 3d, 4d, and 5d transition-metal surfaces depend strongly on the choice of κ. For $\kappa = 0.804$, the atoms and molecules are overbound by 0.2−0.6 eV.[37] Zhang and Yang[38] found that, without violating the Lieb−Oxford bound, the use of $\kappa = 1.245$ (RPBE) gives the best atomization energies for 23 small molecules. Therefore, we further carried out the RPBE single-point energy calculations on the PBE optimized geometries. Compared with PBE, RPBE lowers the hydrogen adsorption energies systemically by about 0.3 eV (Tables 3 and 4). More important, the RPBE-calculated adsorption energy of −0.91 eV at the saturated coverage of 2 ML[30] for the most stable site (tsb/qff, Table 4) is the same as the experimentally determined value.[12] This excellent agreement suggests that RBPE can give sufficient accuracy for the adsorption energies of the H/Fe system. In the following sections, we use the RPBE energies for discussion, and the PBE values are provided for comparison.

2.2. Models. Fe(111) is a steplike or defectlike surface with atoms of both the second and the third layers exposed. The top and side views are shown in Figure 2. The iron atoms of the first, second, and third layers are labeled as Fe1, Fe2, and Fe3, respectively. Both experimental[39] and our previous DFT[40] studies have verified that the very open structure of the clean Fe(111) surface exhibits large multilayer relaxation. For modeling Fe(111), a slab with seven iron layers was employed, in which the top three layers were allowed to relax, while the bottom four layers were fixed in their bulk positions (3Fe/4Fe) to represent the semi-infinite bulk crystal beneath the surface. The free H_2 molecule was placed in a 10-Å cubic box to eliminate the interaction of neighboring H_2 molecules, and the equilibrium bond length of 0.753 Å was obtained (comparable to the experimental value of 0.741 Å[41]). In all calculations, hydrogen was adsorbed only on one side of the Fe slab, and the initial H_2 molecule was put to 1.750 Å above the iron atom (from the low-energy electronic diffraction experiment[42]) with the H−H distance of 0.753 Å.

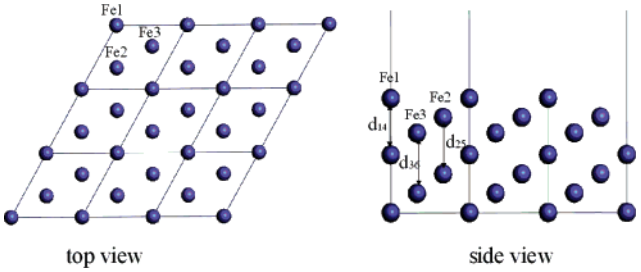

Figure 2. Top view and side view of Fe(111) surface.

TABLE 1: Convergence Tests for Adsorption Energies (E_{ads}, eV) with Relaxation and *k*-points

unit cell	θ	site	nFe$_r$[a]	*k*-point	E_{ads}[b]
$p(1 \times 1)$	2 ML	tsb/qff	3	$7 \times 7 \times 1$	−0.912 (−1.246)
$p(1 \times 1)$	2 ML	tsb/qff	4	$7 \times 7 \times 1$	−0.912 (−1.247)
$p(1 \times 1)$	2 ML	tsb/qff	3	$8 \times 8 \times 1$	−0.912 (−1.242)
$p(2 \times 1)$	1 ML	tsb/tsb-2	3	$7 \times 4 \times 1$	−1.110 (−1.396)
$p(2 \times 1)$	1 ML	tsb/tsb-2	3	$8 \times 5 \times 1$	−1.094 (−1.382)
$p(\sqrt{3} \times \sqrt{3})$	2/3 ML	tsb/tsb-2	3	$4 \times 4 \times 1$	−1.120 (−1.387)
$p(\sqrt{3} \times \sqrt{3})$	2/3 ML	tsb/tsb-2	3	$5 \times 5 \times 1$	−1.104 (−1.377)

[a] Number of the relaxed Fe layers. [b] Values in parentheses are derived from the PBE functional.

Different surface unit cells were used to calculate the adsorption energy of H_2 at different coverage, such as $p(1 \times 1)$ for 2 monolayer (ML), $p(2 \times 1)$ for 1 ML, and $p(\sqrt{3} \times \sqrt{3})$ for 2/3 ML. The adsorption energy per H_2 is defined as $E_{ads} = E(H_2/slab) - [E(slab) + E(H_2)]$, where $E(H_2/slab)$ is the total energy of the slab with one adsorbed hydrogen molecule, $E(slab)$ is the total energy of the corresponding bare Fe slab, and $E(H_2)$ is the total energy of free H_2. Therefore, the more negative the E_{ads}, the stronger the adsorption. The H coverage (θ) is defined as the number of the adsorbed H atoms over the number of the first layer Fe atoms.

The *k*-points were chosen to ensure different surface unit cells having equivalent sampling of Brillouin zones (BZ). Therefore, the *k*-point meshes of $(7 \times 7 \times 1)$, $(7 \times 4 \times 1)$, and $(4 \times 4 \times 1)$ were adopted for $p(1 \times 1)$, $p(2 \times 1)$, and $p(\sqrt{3} \times \sqrt{3})$ unit cells, respectively. To check the rationality of the models, the convergence of the adsorption energy with respect to the number of the relaxed layers and *k*-points was examined. The results are listed in Table 1. For the hydrogen adsorption on the tsb/qff site at 2 ML (**13** in Figure 4), the three-layers relaxed model and four-layers relaxed model give the same H_2 adsorption energy. Increasing the *k*-point meshes from $(7 \times 7 \times 1)$, $(7 \times 4 \times 1)$, and $(4 \times 4 \times 1)$ to $(8 \times 8 \times 1)$, $(8 \times 5 \times 1)$, and $(5 \times 5 \times 1)$ in $p(1 \times 1)$, $p(2 \times 1)$, and $p(\sqrt{3} \times \sqrt{3})$ unit cells, the changes in H_2 adsorption energy are 0.000, 0.016, and 0.016 eV (**13** and **10** in Figure 4, and **3** in Figure 3), respectively. These small energy discrepancies indicate that the three-layers relaxed slabs with $(7 \times 7 \times 1)$, $(7 \times 4 \times 1)$, and $(4 \times 4 \times 1)$

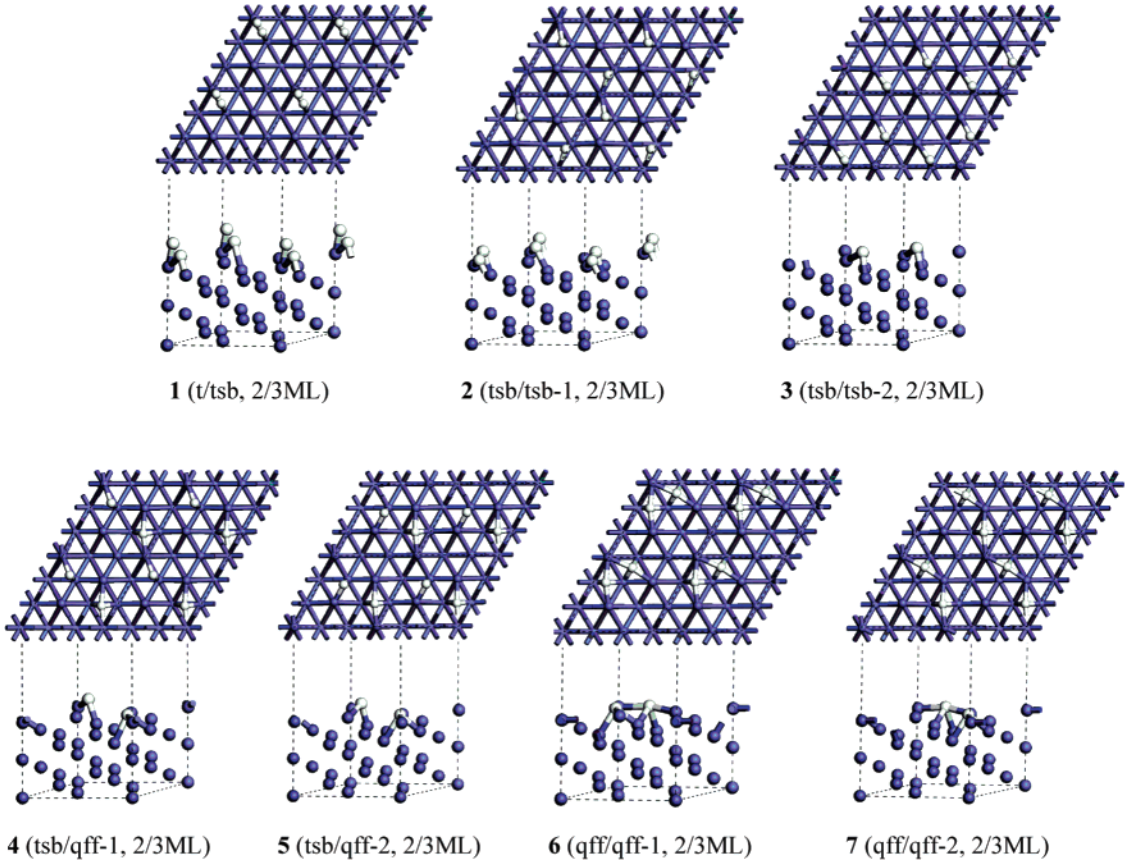

Figure 3. Configurations of hydrogen adsorption on Fe(111) at 2/3 ML (blue: Fe atom; white: H atom).

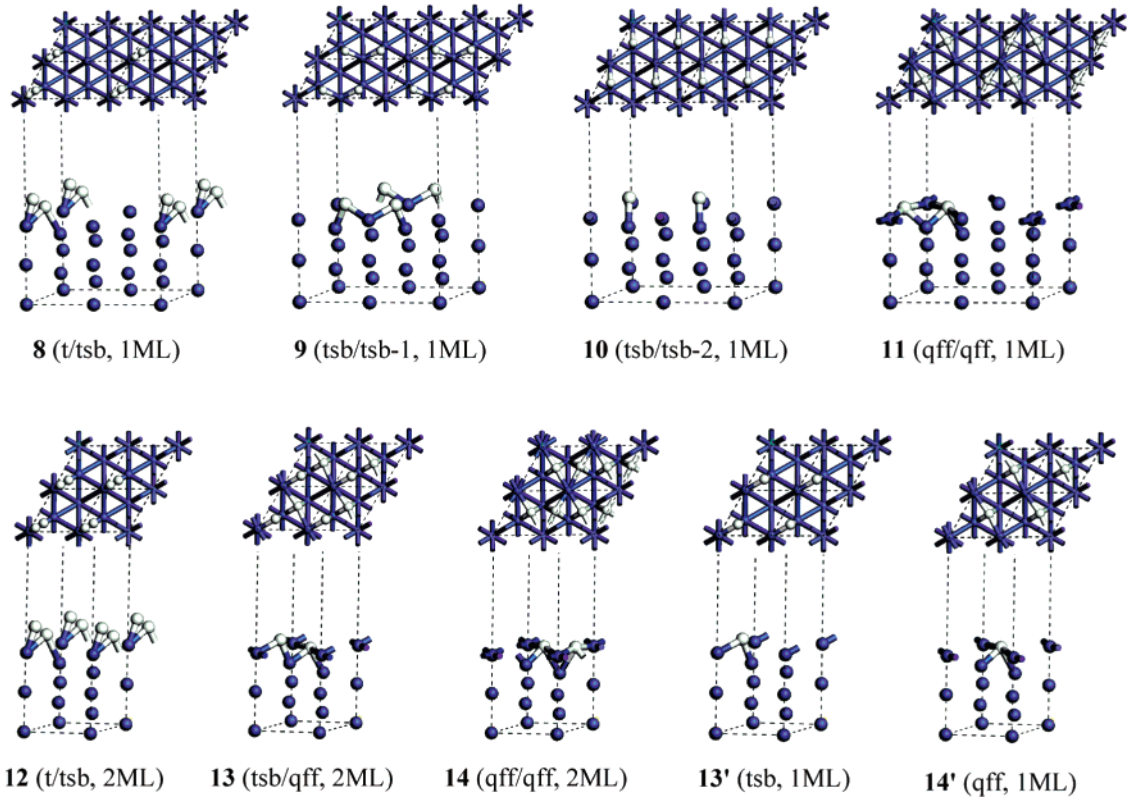

Figure 4. Configurations of hydrogen adsorption on Fe(111) at 1 and 2 ML (blue: Fe atom; white: H atom; **8**−**14** for H_2 adsorption, **13′-14′** for H adsorption).

k-point meshes in $p(1 \times 1)$, $p(2 \times 1)$,and $p(\sqrt{3} \times \sqrt{3})$ unit cells can give sufficient accuracy for the calculation of H_2 adsorption energy. In addition, we have used a similar method and model to investigate the CO adsorption on Fe(111)

TABLE 2: Relaxations of the Clean Fe(111) Surface

	three layers relaxed (%)	four layers relaxed (%)	experiment (%)[a]
$\Delta d_{14}/(3d)$	−3.9	−3.7	-7.5 ± 3.2
$\Delta d_{25}/(3d)$	−3.5	−3.7	-2.6 ± 3.4
$\Delta d_{36}/(3d)$	2.5	2.2	0.7 ± 2.4

[a] From ref 39.

TABLE 3: Calculated Bond Lengths (d, Å) and Adsorption Energies (E_{ads}, eV) for Hydrogen Adsorption on Fe(111) at 2/3 ML

site	E_{ads}[a]	d_{H-H}	d_{H-Fe1}	d_{H-Fe2}	d_{H-Fe3}
1 (t/tsb)	−0.12	1.117	1.585		
	(−0.41)		1.631	1.860	
2 (tsb/tsb-1)	−1.11	3.390	1.819	1.621	
	(−1.38)		1.895	1.619	
3 (tsb/tsb-2)	−1.12	3.811	1.823	1.622	
	(−1.39)		1.821	1.622	
4 (tsb/qff-1)	−1.08	3.719	1.791	1.627	
	(−1.38)		1.894, 2.132	1.673	1.928
5 (tsb/qff-2)	−1.05	3.089	1.825	1.620	
	(−1.35)		1.944, 2.052	1.651	2.019
6 (qff/qff-1)	−0.96	2.369	1.945, 2.056	1.662	1.905
	(−1.31)		1.950, 2.049	1.662	1.907
7 (qff/qff-2)	−0.99	3.463	1.991, 1.996	1.668	1.960
	(−1.33)		1.990, 1.991	1.663	1.986

[a] Values in parentheses are derived from the PBE functional.

successfully.[40] The calculated lattice constant and magnetic moment for α-Fe of 2.826 Å and 2.24 μ_B are in agreement with the experimental values[43] of 2.866 Å and 2.22 μ_B.

3. Results and Discussion

3.1. Clean Fe(111) Surface. The very open structure of the clean Fe(111) surface is known to exhibit large multiplayer relaxation. With d_{ik} being the spacing between the ith and kth atomic layer and d being the bulk spacing, Sokolov et al.[39] found the following relaxations: $\Delta d_{12}/d = (-16.9 \pm 3.0)\%$, $\Delta d_{23}/d = (-9.8 \pm 3.0)\%$, $\Delta d_{34}/d = (4.2 \pm 3.6)\%$, and $\Delta d_{45}/d = (-2.2 \pm 3.6)\%$. The relaxation of our seven-layer slab is shown in Table 2. Here only the three or four topmost layers are relaxed, and the relaxation is tabulated as relative changes in nearest-neighbor distances $\Delta d_{i(i+3)}/3d$ instead of $\Delta d_{i(i+1)}/d$ (Figure 2). The agreement of our calculated results with experimental values further suggests that the employed methods and models are appropriate.

3.2. θ_H = 2/3 ML. As shown in Figure 3, there are seven configurations (**1**−**7**) for hydrogen adsorption on Fe(111) at 2/3 ML, and the calculated bond parameters and adsorption energies are given in Table 3.

Configuration **1** (t/tsb) has H_2 adsorption on the top site. In **1**, H_2 is highly activated, but not dissociated, as indicated by the elongated H−H distance of 1.117 Å. Interestingly, the adsorbed H_2 tilts along the Fe1−Fe2 bond leading to one of the H atoms at the top-shallow bridge site (tsb) with H−Fe distances of 1.631 Å (H−Fe1) and 1.860 Å (H−Fe2), respectively. This suggests that the second-layer Fe atom has a strong interaction with the top adsorbed H_2. In addition, the adsorption energy of **1** (t/tsb) is computed to be −0.12 eV.

In the other cases (**2**−**7**), hydrogen adsorbs dissociatively. Configurations **2** (tsb/ tsb-1) and **3** (tsb/tsb-2) have the adsorbed H atoms at the top-shallow bridge sites (tsb) and differ in their arrangement on the surface. In **2** (tsb/tsb-1), two dissociative H atoms share one first-layer Fe atom, while they occupy the parallel top-shallow bridge sites in **3** (tsb/tsb-2). On the basis of the long H−H distances (3.390 Å in **2** and 3.811 Å in **3**), one can expect that there is no obvious interaction between the H adatoms in **2** (tsb/tsb-1) and **3** (tsb/tsb-2). Therefore, **2** (tsb/tsb-1) and **3** (tsb/ tsb-2) have very close adsorption energies (−1.11 and −1.12 eV, respectively). It is also noteworthy that two H−Fe bonds are not equal in the top-shallow bridge (tsb) form. The H−Fe2 bond is stronger than the H−Fe1 bond in **2** and **3** (∼1.6 vs ∼1.8 Å), while the reversed trend is found for the top-shallow bridge (tsb) form in **1** (1.860 vs 1.631 Å) resulting from the attractive interaction of two nondissociative H atoms. In **4** (tsb/qff-1) and **5** (tsb/qff-2), two dissociative H atoms reside at the top-shallow bridge site (tsb) and the quasi 4-fold site (qff), respectively. For the quasi 4-fold site (qff), H atom bridges over the second (shallow-hollow) and the third layer (deep-hollow) Fe atoms, and ties with two first-layer Fe atoms, forming the subsurface H. Among the four H−Fe bonds, there is a short bond of ∼1.6 Å (H−Fe2) and three longer ones of ∼2.0 Å (H−Fe3 and H−Fe1). These bond parameters indicate again that the second-layer Fe atom has stronger interaction with the atomic H than the first-layer and third-layer Fe atoms. Despite the fact that H atoms exhibit different arrangements on the surface, **4** (tsb/qff-1) and **5** (tsb/qff-2) have close adsorption energies (−1.08 and −1.05 eV). Configurations **6** (qff/qff-1) and **7** (qff/qff-2) illustrate the adsorbed H atoms at the quasi 4-fold sites (qff). In **6** (qff/qff-1), two dissociative H atoms share one of the first-layer Fe atoms and bond to the same second-layer Fe atom, while the H adatoms of **7** (qff/qff-2) form the parallel chains inserting in the Fe(111) surface. As expected, **6** (qff/qff-1) and **7** (qff/qff-2) also have close adsorption energies (−0.96 and −0.99 eV).

TABLE 4: Calculated Bond Lengths (d, Å) and Adsorption Energies (E_{ads}, eV) for Hydrogen Adsorption on Fe(111) at 1 and 2 ML

site	E_{ads}[a]	d_{H-H}	d_{H-Fe1}	d_{H-Fe2}	d_{H-Fe3}
		1 ML			
8 (t/tsb)	−0.13	0.987	1.620		
	(−0.41)		1.649	1.980	
9 (tsb/tsb-1)	−1.09	3.133	1.814	1.616	
	(−1.38)		1.814	1.616	
10 (tsb/tsb-2)	−1.11	3.920	1.801	1.621	
	(−1.40)		1.799	1.622	
11 (qff/qff)	−1.00	2.423	1.920, 2.120	1.674	1.890
	(−1.35)		1.954, 2.041	1.662	1.907
		2 ML			
12 (t/tsb)	−0.17	0.953	1.639		
	(−0.44)		1.665	2.018	
13 (tsb/qff)	−0.91	2.159	1.761	1.615	
	(−1.25)		1.993, 2.026	1.633	1.826
14 (qff/qff)	−0.81	2.078	1.897, 2.130	1.612	2.018
	(−1.17)		1.986, 2.045	1.604	2.047

[a] Values in parentheses are derived from the PBE functional.

From the energy data in Table 3, we can see that all dissociated adsorption states at 2/3 ML are close in energy with the largest discrepancy of 0.16 eV, and thus **2**−**7** should coexist. In contrast, **1** (t/tsb) for the activated adsorption is 1.00 eV higher in energy, and therefore not competitive. Although there are seven configurations (**1**−**7**) for H_2 adsorption on Fe(111) at 2/3 ML, the adsorption sites for the H atom are only three, that is, the top site (t), the top-shallow bridge site (tsb), and the quasi 4-fold site (qff) (Figure 1). The top-shallow bridge site (tsb) is the most stable site, followed by the quasi 4-fold site (qff) and the top site (t). However, the proposed deep-hollow and the shallow-hollow sites by Bernasek et al.[30] are not found in this study. All geometry optimizations to locate the H atom at the deep-hollow site or the shallow-hollow site eventually result in the quasi 4-fold (qff) or the top-shallow bridge (tsb) adsorption.

3.3. $\theta_H = 1$ and 2 ML. Next, we pay attention to the effects of the coverage on the adsorption configurations and adsorption energies. The optimized structures of hydrogen adsorption on Fe(111) at 1 and 2 ML are displayed in Figure 4, while the corresponding bond parameters and adsorption energies are given in Table 4.

As shown in Figure 4, hydrogen adsorption on Fe(111) at 1 ML yields four configurations, **8** (t/tsb), **9** (tsb/tsb-1), **10** (tsb/tsb-2), and **11** (qff/qff). **8** (t/tsb), **9** (tsb/ tsb-1), and **10** (tsb/tsb-2) are similar to **1** (t/tsb), **2** (tsb/tsb-1), and **3** (tsb/tsb-2) at 2/3 ML, respectively, while **11** (qff/qff) is a combination of **6** (qff/qff-1) and **7** (qff/ qff-2). No cross configuration with H adatoms at the top-shallow bridge site (tsb) and the quasi 4-fold site (qff) is found at 1 ML.

At the high coverage of 2 ML, only three adsorption configurations, **12** (t/tsb), **13** (tsb/qff), and **14** (qff/qff), are located. For hydrogen adsorption at the tsb/qff sites, the arrangement of H adatoms on the surface is varied with the coverage (**13** at 2 ML vs **4** and **5** at 2/3 ML).

The effect of the coverage on adsorption energies is tightly correlated with the interaction of the H adatoms. On the basis of the multiple scattering theory, Muscat[20] has calculated the interaction energy between H adatoms for the H/Fe(110) system. It was found that the interaction energy mainly derives from the short-range pair interaction, while the contributions of the long-range pair interaction and nonpairwise interaction are in a lower order of magnitude. For the H−H distance in the range of 1.4 to 2.5 Å, there is considerably repulsive interaction between the H adatoms. With the H−H distance increase, this repulsive short-range H−H interaction decreases gradually. When the H−H distance is over 3.5 Å, the H adatoms exhibit the weak attractive interaction.

For hydrogen adsorption on Fe(111) at the tsb/tsb sites, the H_2 is dissociated at 2/3 and 1 ML with the H−H distances of 3.390/3.811 Å and 3.133/3.920 Å, respectively (Tables 3 and 4). In these cases, the interaction between H adatoms is very weak. Therefore, the coverage effect is negligible, as indicated by the very close geometric structures and adsorption energies of the corresponding configurations (**2** and **3** at 2/3 ML with respect to **9** and **10** at 1 ML, respectively). Compared with the tsb/tsb sites, the distance between two dissociative H atoms at the qff/qff sites is small, such as 2.369 Å for **6** at 2/3 ML, 2.423 Å for **11** at 1 ML, and 2.078 Å for **14** at 2 ML. In this scope, the repulsive short-range H−H interaction should be strong. In accord with the tendency of the H−H distance, the adsorption energy for **11** at 1 ML is slightly stronger than that for **6** at 2/3 ML (−1.00 vs −0.96 eV). At the coverage of 2 ML (**14**), the adsorption energy decreases greatly (−0.81 eV). A similar case is also found for hydrogen adsorption at the tsb/qff sites. However, the case for hydrogen adsorption at the t/tsb site is remarkably different. Due to the adsorbed H_2 in an activated but nondissociated state, the attractive interaction should exist between two H adatoms. The shorter the H−H bond, the stronger the attractive interaction. Note that with the coverage increase, the H−H bond length decreases from 1.117 Å (2/3 ML) to 0.987 Å (1 ML) and then to 0.953 Å (2 ML). On this basis, we can conclude that the attractive short-range H−H interaction results in an increase of the adsorption energy as the coverage changing from 2/3 to 2 ML. On the other hand, the H−Fe interaction is reduced at increased coverage (1.585/1.631 at 2/3 ML, 1.620/1.649 at 1 ML, and 1.639/1.665 Å at 2 ML, respectively), which leads to a decrease of the adsorption energy. Rising from these opposite effects, the t/tsb configuration has the very close adsorption energy at 2/3 ML (−0.12 eV) and 1 ML (−0.13 eV), while a slightly stronger adsorption energy of −0.17 eV at 2 ML.

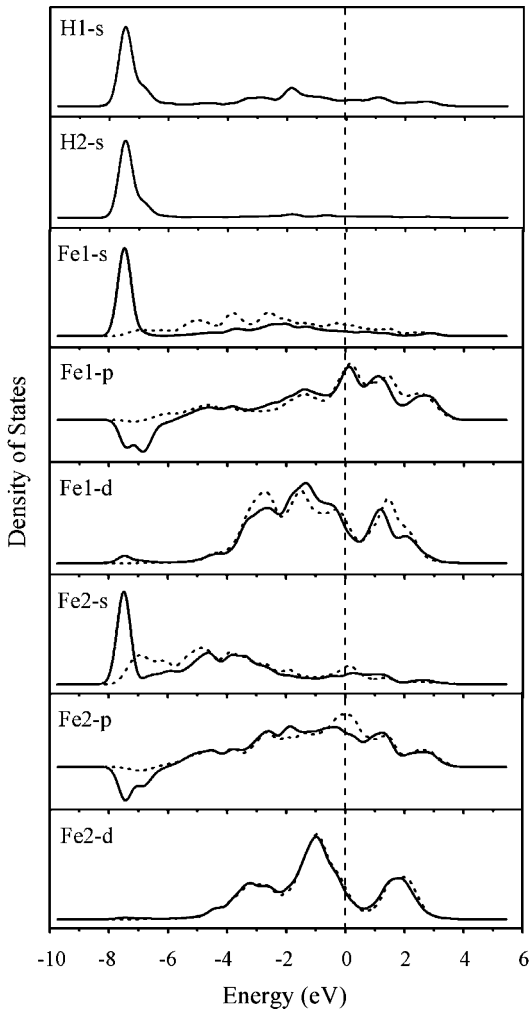

Figure 5. LDOS for adsorbed H and surface Fe atoms of H/Fe(111) at 2/3 ML (**1**): H1 on the top site (t); H2 on the top-shallow bridge site (tsb) (solid lines for bands after adsorption, dashed line for bands before adsorption).

3.4. Comparison with Experiment. In an early experimental study by Bozso et al.,[12] it was observed that the thermal desorption spectroscopy (TDS) from H/Fe(111) at saturated coverage has three desorption states, β_1, β_2, and β_3, corresponding to the temperature of 220, 300, and 360 K, respectively. On the basis of the TDS plot, they obtained an initial adsorption energy of −0.91 eV. In comparison, our RPBE-calculated value of −0.91 eV for hydrogen adsorption on the most stable site (tsb/qff) at the saturated coverage of 2 ML[30] is in excellent agreement with the experiment.

Furthermore, the second-order plot for the desorption kinetics of the β_1, β_2, and β_3 states yielded desorption energies of 0.56, 0.78, and 0.91 eV, respectively.[12] The adsorption energies in Table 4 clearly show that at 2 ML, hydrogen adsorbs dissociatively in **13** (tsb/qff) and **14** (qff/qff), and **13** is more favored by 0.10 eV. This shows that the desorption sequence depends on the adsorption of H adatom. To assign the desorption order, we have examined the adsorbed site with one atomic hydrogen at the top-shallow bridge site (tsb, **13′**) and the quasi 4-fold site (qff, **14′**) on $p(1 \times 1)$ unit cell (Figure 4), which mimic those in **13** and **14**; the calculated adsorption energies[27] for **13′** (tsb) and **14′** (qff) are −0.55 and −0.51 eV per H atom, respectively. As a consequence, H atoms at the quasi 4-fold site (qff) desorb prior to those at the top shallow bridge site

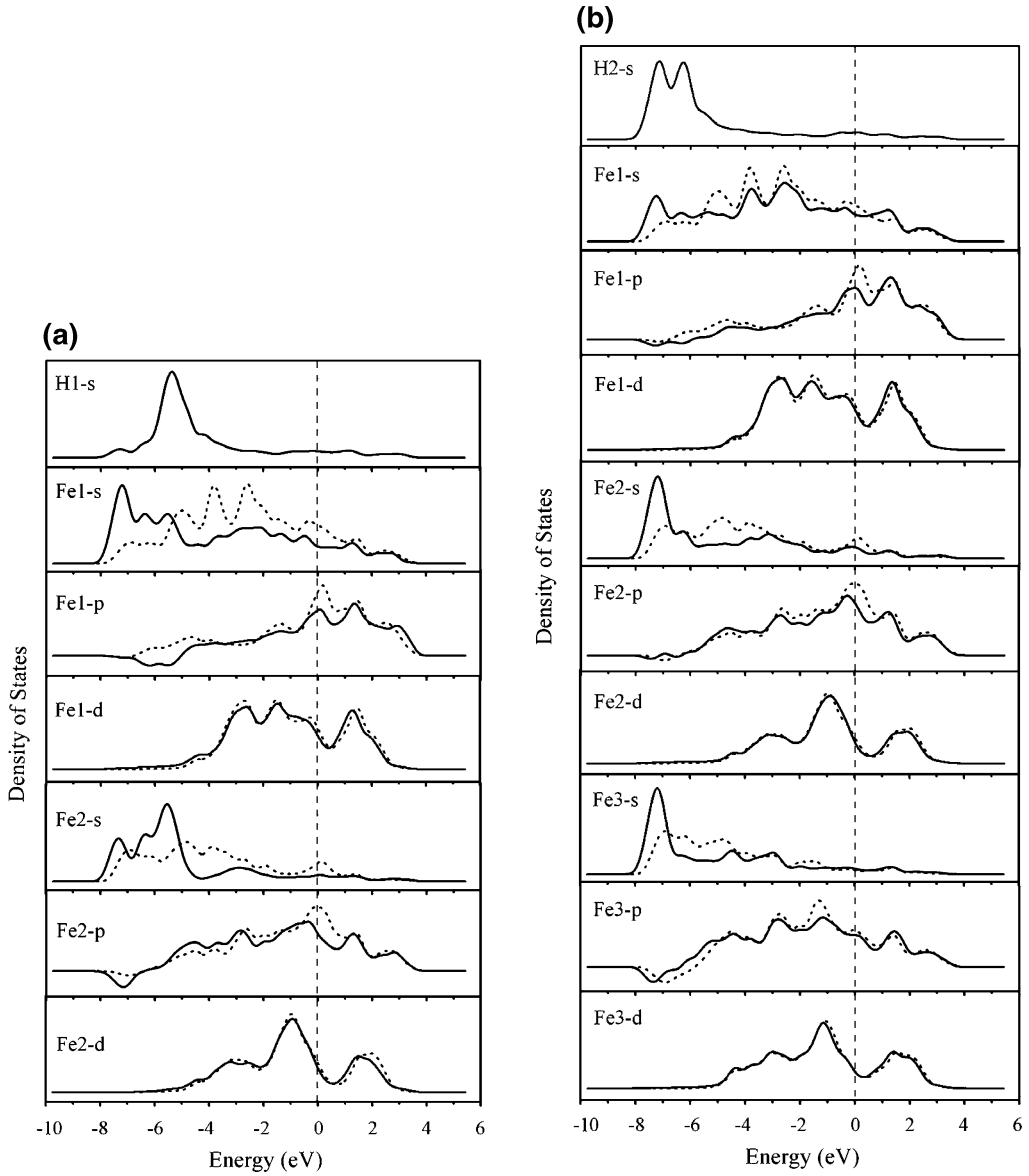

Figure 6. LDOS for adsorbed H and surface Fe atoms of H/Fe(111) at 2/3 ML (**4**): (a) H1 on the top-shallow bridge site (tsb); (b) H2 on the quasi 4-fold site (qff) (solid lines for bands after adsorption, dashed line for bands before adsorption).

(tsb). It is also noteworthy that H−H interaction has an influence on the H desorption at higher coverage, and H desorption is accompanied with H diffusion from the quasi 4-fold site (qff) to the more favored top-shallow bridge site (tsb).[12] On the basis of the above consideration, we have calculated the stepwise desorption energies (E_d) of **13** (tsb/qff) and **14** (qff/qff), as shown in eqs 1−3. The relative order of the calculated desorption energies shows that the β_1, β_2, and β_3 desorption states correspond to the quasi 4-fold site (qff) of the qff/qff configuration (0.60 eV), the quasi 4-fold site (qff) of the tsb/qff configuration (0.74 eV), and the top-shallow bridge site (1.10 eV), respectively. These agreements in turn confirm that our proposed adsorption sites should be reliable.

$$\mathbf{14}\ (\text{qff/qff}) \rightarrow \mathbf{14'}\ (\text{qff}) + \text{H}_2 \quad E_d = 0.60\ \text{eV} \qquad (1)$$

$$\mathbf{13}\ (\text{tsb/qff}) \rightarrow \mathbf{13'}\ (\text{tsb}) + \text{H}_2 \quad E_d = 0.74\ \text{eV} \qquad (2)$$

$$\mathbf{13'}\ (\text{tsb}) \rightarrow \text{Fe (bare)} + \text{H}_2 \quad E_d = 1.10\ \text{eV} \qquad (3)$$

3.5. Electronic Structure and Density of States. To understand the nature of the bonding between H and Fe(111), a detailed analysis of electronic structures with the local density of states (LDOS) was carried out. The LDOS for the adsorbed H atoms and the surface Fe atoms for the top site (t), the top-shallow bridge site (tsb), and the quasi 4-fold site (qff) at 2/3 ML are shown in Figures 5 and 6, respectively.

The LDOS in Figure 5 represents the hydrogen adsorption on the t/tsb site, in which H_2 is highly activated with the H atoms occupying the top site (t) and the top-shallow bridge site (tsb), respectively. We can see that the peak of the H 1s band is very sharp at about −7.4 eV below the Femi level (E_F). When H_2 adsorbs on the t/tsb site, the H 1s band has a strong interaction with the 4s, 4p, and 3d bands of the first-layer Fe atom (Fe1) as well as the 4s and 4p bands of the second-layer Fe atom (Fe2), as indicated by the large changes of the Fe1 4s, 4p, and 3d as well as the Fe2 4s and 4p with respect to the bare Fe surface.

However, the case for H dissociated adsorption is clearly different. As illustrated in Figure 6, the H 1s band for the top-shallow bridge site (tsb) is very broad and is centered about −5.4 eV below E_F, while the corresponding band for the quasi 4-fold site (qff) splits into two peaks at −7.2 and −6.3 eV below

E_F. In addition, whether H adatom at the top-shallow bridge site (tsb) or quasi 4-fold site (qff), there is no obvious change in Fe 3d compared to the bare Fe surface. In these cases, the Fe atoms mainly utilize 4s and 4p electrons bonding to a H atom, with small contributions from the 3d electrons. A similar bonding picture has been proposed in previous studies.[23,44−47] They found that the bridge or hollow site adsorption mainly uses more delocalized interstitial electrons of sp character, while due to its more localized nature, the top adsorption involves the localized d-orbital.

3.6. Diffusion of the H Adatom. At this stage, it is necessary and interesting to discuss the H adatom diffusion on Fe(111) between different adsorption sites, such as from the top site (t) to the top-shallow bridge site (tsb) and from the top-shallow bridge site (tsb) to the quasi 4-fold site (qff). A $p(\sqrt{3} \times \sqrt{3})$ unit cell was employed, and two corresponding transition states were located.

Since the adsorbed H_2 is not dissociated at the t/tsb site, we adopt configurations **1** (t/tsb) and **2** (tsb/tsb-1) to discuss the diffusion of the H adatom between the top site (t) and the top-shallow bridge site (tsb). The structure of the corresponding transition state is very close to that of **1** (t/tsb). Compared with **1** (t/tsb), the main change in transition state is the elongated H−H bond (1.194 vs 1.117 Å). The H adatoms diffuse from the t/tsb site to the tsb/tsb-1 site without any barrier, while an energy barrier of 0.99 eV is found for the reverse course. For the H adatom diffusion between the top-shallow bridge site (tsb) and the quasi 4-fold site (qff), the geometry of the transition state is very similar to that of the H adatom at the quasi 4-fold site (qff). The corresponding diffusion energy barriers for both directions are very small, that is, 0.08 eV for the top-shallow bridge site (tsb) to the quasi 4-fold site (qff) and 0.01 eV for the reverse course. These energy data suggest that the H adatoms have a large mobility on Fe(111), in line with the experimental observations.[12,30]

4. Conclusion

Hydrogen adsorption on Fe(111) at a set of coverages has been investigated at the level of density functional theory. It is found that there are three adsorption sites for H atom, that is, the top site (t), the top-shallow bridge site (tsb), and the quasi 4-fold site (qff). At all coverages, the most favored adsorption site is the top-shallow bridge site (tsb), followed by the quasi 4-fold site (qff) with an energy difference of less than 0.1 eV, while the top site (t) is higher in energy and not competitive. For hydrogen adsorption at the t/tsb site, H_2 is highly activated, but not dissociated. In the other cases, the hydrogen adsorbs dissociatively. Furthermore, the small diffusion barriers indicate that the H adatoms have a large mobility on the Fe(111) surface.

The coverage effect on the adsorption energies is complicated. For hydrogen adsorption at the tsb/tsb sites, the adsorption energy has no obvious difference between 2/3 and 1 ML, indicating that the interaction of the H adatoms is very weak and negligible. For hydrogen adsorption at the qff/qff sites, the H−H distance becomes shorter at about 2.0−2.5 Å. Rising from the repulsive short-range H−H interaction, the adsorption energy at 1 ML is slightly stronger than that at 2/3 ML, and it decreases largely at 2 ML. However, the trend for hydrogen activated adsorption at the t/tsb site is considerably different. Due to the effects of the attractive short-range H−H interaction and the H−Fe interaction, the adsorption energies at 2/3 and 1 ML are close, while it increases slightly at 2 ML. In addition, the RPBE-calculated adsorption energy of −0.91 eV at the saturation coverage of 2 ML for the tsb/qff site is in excellent agreement with experiment.

The LDOS analysis reveals that the principal contributions to the Fe−H (tsb or qff) bond are from the Fe 4s and 4p and H 1s orbitals, and to a lesser extent the Fe 3d orbital. Nevertheless, the Fe 4s, 4p, and 3d orbitals have a strong interaction with the H (top) 1s orbital.

Acknowledgment. We thank the National Natural Science Foundation of China (Grants No. 20473111 and No. 20590361) and Chinese Academy of Sciences (2004908) as well as State Key Laboratory of Coal Conversion, Institute of Coal Chemistry (04-908) for financial support.

References and Notes

(1) (a) Christmann, K. *Surf. Sci. Rep.* **1988**, *9*, 1. (b) Christmann, K. *Prog. Surf. Sci.* **1995**, *48*, 15.
(2) Myers, S. M.; Baskes, M. I.; Birnbaum, H. K.; Corbett, J. W.; De Leo, G. G.; Estreicher, S. K.; Haller, E. E.; Jena, P. N.; Johnson, N. M.; Kirchheim, R.; Pearton, S. J.; Stavola, M. J. *Rev. Mod. Phys.* **1992**, *64*, 559.
(3) Müller, K. *Prog. Surf. Sci.* **1993**, *42*, 245.
(4) Watson, G. W.; Wells, R. P. K.; Willock, D. J.; Hutchings, G. J. *J. Phys. Chem. B* **2001**, *105*, 4889.
(5) Paul, J. F.; Sautet, P. *Surf. Sci. Lett.* **1996**, *356*, L403.
(6) Ciobîcã, I. M.; Kleyn, A. W.; van Santen, R. A. *J. Phys. Chem. B* **2003**, *107*, 164.
(7) Kinke, D. J., II; Broadbelt, L. J. *Surf. Sci.* **1999**, *429*, 169.
(8) Anderson, R. B. *The Fischer−Tropsch Synthesis*; Academic Press: Orlando, FL, 1984.
(9) Somorjai, G. A. *Introduction to Surface Chemistry and Catalysis*; John Wiley & Sons: New York, 1994.
(10) Zhong, W.; Cai, Y.; Tomanek, D. *Nature* **1993**, *362*, 435.
(11) Wang, J.-S. *Eng. Fract. Mech.* **2001**, *68*, 647.
(12) Bozso, F.; Ertl, G.; Grunze, M.; Weiss, M. *Appl. Surf. Sci.* **1977**, *1*, 103.
(13) Weiss, M.; Ertl, G.; Nitschke, F. *Appl. Surf. Sci.* **1979**, *2*, 614.
(14) Imbihl, R.; Behm, R. J.; Christmann, K.; Ertl, G.; Matsushima, T. *Surf. Sci.* **1982**, *117*, 257.
(15) Moritz, W.; Imbihl, R.; Behm, R. J.; Ertl, G.; Matsushima, T. *J. Chem. Phys.* **1985**, *83*, 1959.
(16) Nichtl-Pecher, W.; Gossmann, J.; Hammer, L.; Heinz, K.; Müller, K. *J. Vac. Sci. Technol. A* **1992,** *10*, 501.
(17) Hammer, L.; Landskron, H.; Nichtl-Pecher, W.; Fricke, A.; Heinz, K.; Müller, K. *Phys. Rev. B* **1993**, *47*, 15969.
(18) Raeker, T. J.; DePristo, A. E. *Surf. Sci.* **1990**, *235*, 84.
(19) Cremaschi, P.; Yang, H.; Whitten, J. L. *Surf. Sci.* **1995**, *330*, 255.
(20) Muscat, J. P. *Surf. Sci.* **1984**, *139*, 491.
(21) Muscat, J. P. *Surf. Sci.* **1982**, *118*, 321.
(22) Eder, M.; Terakura, K.; Hafner, J. *Phys. Rev. B* **2001**, *64*, 115426.
(23) Jiang, D. E.; Carter, E. A. *Surf. Sci.* **2003**, *547*, 85.
(24) Merrill, P. B.; Madix, R. J. *Surf. Sci.* **1996**, *347*, 249.
(25) Walch, S. P. *Surf. Sci.* **1984**, *143*, 188.
(26) Eder, M.; Terakura, K.; Hafner, J. *Phys. Rev. B* **2002**, *64*, 115426.
(27) Jiang, D. E.; Carter, E. A. *Phys. Rev. B* **2004**, *70*, 064102.
(28) Schmiedl, R.; Nichtl-Pecher, W.; Hammer, L.; Heinz, K.; Müller, K. *Surf. Sci.* **1995**, *324*, 289.
(29) Spence, N. D.; Schoonmaker, R. C.; Somorjai, G. A. *J. Catal.* **1982**, *74*, 129.
(30) Bernasek, S. L.; Zappone, M.; Jiang, P. *Surf. Sci.* **1992**, *272*, 53.
(31) Berger, H. F.; Rendulic, K. D. *Surf. Sci.* **1991**, *251/252*, 882.
(32) (a) Payne, M. C.; Allan, D. C.; Arias, T. A.; Joannopoulos, J. D. *Rev. Mod. Phys.* **1992**, *64*, 1045. (b) Milman, V.; Winkler, B.; White, J. A.; Pickard, C. J.; Payne, M. C.; Akhmataskaya, E. V.; Nobes, R. H. *Int. J. Quantum Chem.* **2000**, *77*, 895.
(33) Perdew, J. P.; Burke, S.; Ernzerhof, M. *Phys. Rev. Lett.* **1996**, 77, 3865.
(34) White, J. A.; Bird, D. M. *Phys. Rev. B* **1994**, *50*, 4954.
(35) Vanderbilt, D. *Phys. Rev. B* **1990**, *41*, 7892.
(36) (a) Nayak, S. K.; Nooijen, M.; Bernasek, S. L. *J. Phys. Chem. B* **2001**, *105*, 164. (b) Cheng, H. S.; Reiser, D. B.; Dean, S. W., Jr.; Baumert, K. *J. Phys. Chem. B* **2001**, *105*, 12547. (c) Ge, Q.; Jenkins, S. J.; King, D. A. *Chem. Phys. Lett.* **2000**, *327*, 125.
(37) Hammer, B.; Hansen, L. B.; Nørskov, J. K. *Phys. Rev. B* **1999**, *59*, 7413.
(38) Zhang, Y.; Yang, W. *Phys. Rev. Lett.* **1998**, *80*, 890.
(39) Sokolov, J.; Jona, F.; Marcus, P. M. *Phys. Rev. B* **1986**, *33*, 1397.

(40) Chen, Y.-H.; Cao, D.-B.; Yang, J.; Li, Y.-W.; Wang, J. G.; Jiao, H. *Chem. Phys. Lett.* **2004**, *400*, 35.
(41) Huber, K. P.; Herzberg, G. *Molecular Spectra and Molecular Structure 4: Constants of Diatomic Molecules*; Van Norstrand Reinhold Co.: New York, 1979.
(42) Moritz, W.; Imbihl, R.; Behm, R. J.; Ertl, G.; Matsushima, T. *J. Chem. Phys.* **1985**, *83*, 1959.
(43) Kittel, C. *Introduction to Solid State Physics*; Wiley: New York, 1996.
(44) Juan, A.; Hoffmann, R. *Surf. Sci.* **1999**, *421*, 1.
(45) McAdon, M. H.; Goddard, W. A., III. *J. Phys. Chem.* **1987**, *91*, 2607.
(46) Li, M.; Goddard, W. A., III. *Phys. Rev. B* **1989**, *40*, 12155.
(47) Li, M.; Goddard, W. A., III. *J. Chem. Phys.* **1993**, *98*, 7995.